Chemical Research in Toxicology

Article

pubs.acs.org/crt

Molecular Signatures Associated with Treatment of Triple-Negative MDA-MB231 Breast Cancer Cells with Histone Deacetylase Inhibitors JAHA and SAHA

Mariangela Librizzi,[†] Fabio Caradonna,*[,†] Ilenia Cruciata,[†] Janusz Dębski,[‡] Supojjanee Sansook,[§] Michał Dadlez,[‡] John Spencer,[§] and Claudio Luparello[†]

[†]Dipartimento di Scienze e Tecnologie Biologiche, Chimiche e Farmaceutiche (STEBICEF), Università di Palermo, Viale delle Scienze, 90128 Palermo, Italy

[‡]Institute of Biochemistry and Biophysics, Polish Academy of Sciences, Pawinskiego 5a, 02-106 Warsaw, Poland

[§]Department of Chemistry, School of Life Sciences, University of Sussex, Falmer, Brighton BN1 9QJ, United Kingdom

ABSTRACT: Jay Amin hydroxamic acid (JAHA; N8-ferrocenylN[1]-hydroxy-octanediamide) is a ferrocene-containing analogue of the histone deacetylase inhibitor (HDACi) suberoylanilide hydroxamic acid (SAHA). JAHA's cytotoxic activity on MDA-MB231 triple negative breast cancer (TNBC) cells at 72 h has been previously demonstrated with an IC_{50} of 8.45 μM. JAHA's lethal effect was found linked to perturbations of cell cycle, mitochondrial activity, signal transduction, and autophagy mechanisms. To glean novel insights on how MDA-MB231 breast cancer cells respond to the cytotoxic effect induced by JAHA, and to compare the biological effect with the related compound SAHA, we have employed a combination of differential display-PCR, proteome analysis, and COMET assay techniques and shown some differences in the molecular signature profiles induced by exposure to either HDACis. In particular, in contrast to the more numerous and diversified changes induced by SAHA, JAHA has shown a more selective impact on expression of molecular signatures involved in antioxidant activity and DNA repair. Besides expanding the biological knowledge of the effect exerted by the modifications in compound structures on cell phenotype, the molecular elements put in evidence in our study may provide promising targets for therapeutic interventions on TNBCs.

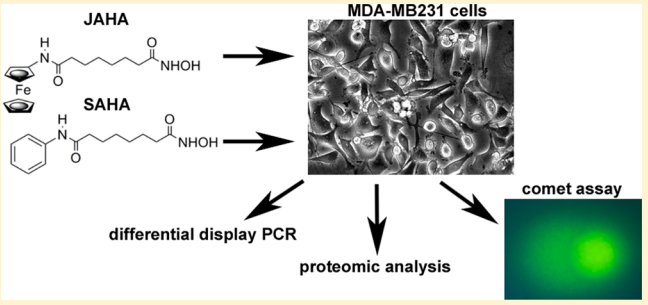

INTRODUCTION

Histone deacetylase inhibitors (HDACis) are chemically heterogeneous promising anticancer agents that restore a relaxed, hyperacetylated chromatin structure and potentially lead to re-expression of silenced genes or silencing of downstream genes, ultimately inducing death, apoptosis, and cell cycle arrest in cancer cells also via non histone-targeted mechanisms such as perturbations of p53, cytokine signaling pathways, and angiogenesis (e.g., ref 1). HDACis are grouped into different categories on the basis of their chemical nature, and the consequence of this molecular diversity is that the precise mechanism through which these compounds work is still poorly understood.

Suberoylanilide hydroxamic acid (SAHA), that is, Vorinostat, is a prototypical HDACi targeting class I and II HDAC approved in 2006 by the Food and Drug Administration for treatment of cutaneous T-cell lymphoma.[2] A number of studies have focused on the understanding of the biological properties of the compound as an anticancer agent, especially against tumors with intrinsic highly malignant potential. Triple-negative breast cancer (TNBC) is a tumor histotype, which is poorly responsive to hormonal therapies and to HER2-targeting drugs and usually associated with worse prognosis than other breast cancers. It is therefore very important to develop and test novel drugs or analogues of pre-existing drugs that counteract TNBC cell growth. In this context, drugs targeting multiple signaling pathways and epigenetic drugs appear to be the most promising.[3] Exposure of TNBC MDA-MB231 cells to SAHA was found to determine the modification of selected gene expression patterns, the disruption of transduction signaling, and the onset of apoptosis.[4−7]

Several manipulations of the core structure of SAHA have been carried out to probe the effect of such SAR (structure activity relationships) modifications on both HDAC inhibitory activity and cytotoxic effects on cancer cells (e.g., ref 8). HDACis typically contain a cap (often aryl group), a linker, and a zinc-binding group. Spencer et al.[9] reported the synthesis of metal-based SAHA analogues that contain a ferrocene cap that are air stable and readily modifiable synthetically such as Jay Amin hydroxamic acid (JAHA). If compared with parental SAHA, JAHA displays similar broad inhibitory profiles toward class I HDACs, including HDAC8, whereas it is inactive on class IIa HDACs. Indeed, many studies have shown that the

Received: September 28, 2017
Published: November 12, 2017

DOI: 10.1021/acs.chemrestox.7b00269
Chem. Res. Toxicol. 2017, 30, 2187−2196

introduction of a ferrocene motif can lead to significant changes in bioactivity not only due to its size and shape, which may alter interactions with crucial residues in active sites for example, but also due to its potential for redox activity (Fe(II)/Fe(III) and induction of reactive oxygen species.[10−14]

Given its different structure, this new compound underwent further study, and in a previous set of experimental assays its ability to counteract TNBC MDA-MB231 cell growth and the related biological aspects were tested. JAHA exhibited a remarkable activity on cell viability and proliferation with an IC_{50} of 8.45 μM at 72 h. In particular, JAHA's cytotoxic activity implied (i) cell cycle perturbation, likely related to an inability of cells to proceed through the G_2/M transition, (ii) an early increase of reactive oxygen species production followed by dissipation of mitochondrial transmembrane potential, and (iii) the inhibition of the autophagic process that plays a pro-survival role in this cell line. Noteworthy, JAHA did not induce the onset of apoptosis that was instead promoted by the archetypal SAHA at the same concentration.[4] Contrary to JAHA, SAHA was proven to enhance the autophagic process in different model systems (e.g., ref 15). Moreover, dealing with survival-related signal transduction pathways, Librizzi et al.[16] reported that, differently from SAHA, JAHA induced the deactivation of pERK1/2, leaving pAKT levels unaltered in MDA-MB231 cells. The resulting inhibition of DNMT1 and DNMT3b methyltransferase activity resulted in a generalized DNA demethylation following JAHA treatment with consequent implications in transcriptional regulation and gene expression pattern.

These cumulative results highlighted a modification of the biological effect consequent to the manipulation of the original molecular structure. It is widely acknowledged that the characterization of the biological activity of new potential anticancer compounds, such as ferrocene-based SAHA analogues, is necessary to establish drug safety and efficacy profiles. In addition, information on the mode of action of the different HDACis may reveal new molecular targets of putative applicative interest, which ultimately may be useful in the design of more appropriate intervention and therapies for tumors with inherent aggressive biology and limited treatment options such as TNBCs. To get novel insight on how MDA-MB231 breast cancer cells respond to the cytotoxic effect induced by JAHA, and to compare the biological effect of the related compounds JAHA and SAHA, we have employed a combination of differential display-PCR, proteome analysis, and Comet assay techniques and shown different molecular signature profiles induced by exposition to either HDACis. As well as expanding the biological knowledge of the effect exerted by the modifications in compound structures on cell phenotype, the molecular elements put in evidence in our study may provide promising targets for therapeutic interventions on TNBCs.

EXPERIMENTAL PROCEDURES

Cells and Treatments. MDA-MB231 breast tumor cells were maintained in RPMI 1640 medium plus 10% fetal bovine serum, 100 U/mL penicillin, 100 μg/mL streptomycin, and 2.5 mg/L amphotericin B (Invitrogen, Carlsbad, CA, USA), at 37 °C in a 5% CO_2 atmosphere. The cells were detached from flasks with 0.05% trypsin-EDTA, counted, and plated at the necessary density for treatment after achieving 60−80% confluency. The HDACis SAHA and JAHA, the latter synthesized as reported in Spencer at al.,[9] were dissolved in dimethyl sulfoxide as stock solutions. Cells (1×10^6) were plated in 75 cm^2 flasks and allowed to adhere overnight. Then the cells were treated with either JAHA or SAHA at 8.45 μM concentration or with the vehicle for 18, 24, and 48 h.

Messenger RNA Isolation and Reverse Transcription. Isolation of total RNA from monolayers of trypsinized control and HDACi-exposed cells and reverse transcriptase reaction were performed with TRIzol reagent (Invitrogen) as described by Sirchia and Luparello.[17] Messenger RNA-enriched samples from total RNA preparations were obtained using Terminator 5′-phosphate-dependent exonuclease (Epicenter, Madison, WI, USA) following manufacturer's instructions, and the mRNA preparations were purified from excess EDTA, tRNA, 5S rRNA, and other small RNA species by LiCl precipitation. The cDNAs were synthesized from 250 ng of mRNA in the presence of random hexamer primers using Superscript II reverse transcriptase (Invitrogen), and their quality was checked by amplification of "housekeeping" β-actin cDNA.

Differential Display (DD) and Real Time-PCR. For differential expression analysis, DD-PCR experiments were performed as already reported (e.g., refs 18 and 19) using 25 pmol of the arbitrary 10-mer primers designed by Sokolov and Prokop,[20] in combinations of two, and 3.6 U of AmpliTaq DNA polymerase, Stoffel fragment (Applied Biosystems/Life Technologies, Carlsbad, CA, USA). The amplification products were checked by nondenaturing 6% polyacrylamide gel electrophoresis (PAGE), performed in a Sequi-Gen sequencing apparatus (Bio-Rad, Hercules, CA, USA) at constant 55 W, and silver staining. The 50 bp DNA Ladder (Invitrogen) was run in parallel for reference and the evaluation of band size performed with SigmaGel software (SPSS, Blairgowrie, UK). The DD-bands of interest were scratched from the gel and used as template for repeated cycles of amplification and electrophoresis until a single pure band was visualized. Then the PCR products were first purified using the Montage PCR Centrifugal Filter Devices (Millipore, Billerica, MA, USA) followed by treatment with ExoSAP-IT (USB, Cleveland, OH, USA) to remove any unconsumed dNTPs and primers remaining in the PCR product mixture, which could interfere with the sequencing reaction. The purified PCR products were submitted for sequencing by BMR Genomics (Padova, Italy) and DNA sequence similarity was searched with the Nucleotide BLAST algorithm available online.

Messenger RNA expression levels were evaluated by quantitative real-time PCR using Power SYBR Green PCR Master Mix (Applied Biosystems, Philadelphia, PA, USA) as previously described[21] in a 7300 Real Time PCR system (Applied Biosystems) in the presence of 2.5 μM of the primers listed in Table 1 and designed using the Primer3 software available at http://biotools.umassmed.edu/bioapps/primer3_www.cgi. Either GAPDH or β-actin was used as internal control. The PCR data obtained were automatically analyzed by the Relative Quantification Study Software (Applied Biosystem) and expressed as target/reference ratio. Thermocycler conditions were 95 °C for 10 min, followed by 40 cycles of 95 °C for 1 min, and 60 °C for 1 min.

Liquid Chromatography−Tandem Mass Spectrometry (LC−MS/MS). Trypsinized control and HDACi-treated cells were dissolved in a solubilization buffer (0.1 M Tris-HCl, pH 8, 25 mM EGTA, 4% SDS, 1X protease inhibitors cocktail, all purchased from Sigma). Then the samples were sonicated, boiled for 3−5 min, and clarified by centrifugation for 15 min at maximum speed after which the supernatant was collected. The proteins were precipitated using 5 volumes of cold acetone (−20 °C), centrifuged at 13 000 rpm for 10 min at 4 °C, and resuspended in 0.1% SDS before sonication. The protein samples were quantified using the BCA assay kit (Thermo Scientific), and 5 μg was used for tryptic digestion and protein identification for quantitative analysis, whereas 24 μg was used for qualitative analysis. Mass spectrometry was performed as reported by Rozek et al.[22] Briefly, the digested peptides were first applied to a RP-18 trapping column (nanoACQUITY UPLC Symmetry C18 Trap, Waters, Milford, MA, USA) using 0.1% trifluoroacetic acid mobile phase and then to a HPLC RP-18 column (nanoACQUITY UPLC BEH C18 Column, Waters) using an acetonitrile gradient (0−30% in 0.1% formic acid), and the column outlet was directly coupled to the ion source of the Ion Cyclotron Resonance spectrometer (LTQ61 FTICR, Thermo Electron). Each sample was submitted to triplicate LC/MS runs followed by analysis on LTQ_OrbitrapVelos (Thermo

DOI: 10.1021/acs.chemrestox.7b00269
Chem. Res. Toxicol. 2017, 30, 2187−2196

Table 1. Sequence of Primers Used for PCR Amplification

transcript detected	product size (bp)	oligonucleotides
PKCε	249	5′-GATCAGAAGGTCACTGCAA-3′
		5′-GTCGTCATGGAGGATGGACT-3′
PKCι	169	5′-TACGGCCAGGAGATACAACC-3′
		5′-TCGGAGCTCCCAACAATATC-3
ERGIC-2	196	5′-GCCATGGAGTCTCTGGGATA-3′
		5′-CCAAGTCTGAAACGACAGCA-3′
RAD50	215	5′-CTTGGATATGCGAGGACGAT-3′
		5′-CCAGAAGCTGGAAGTTACGC-3′
NTRK-2	181	5′-AGCATGAGCACATCGTCAAG-3′
		5′-ATATGCAGCATCTGCGACTG-3′
BIG-3	231	5′-CGCCCTGTCTCTAAAACTGC-3′
		5′-CTGTCTGCGTTCATCAGCAT-3′
VDUP1	223	5′-TTGTTCTCCCCTTCTGCCAT-3′
		5′-AGGGTTGGGCATCTTGATCA-3′
IDI1	206	5′-TTGGGCTGGATAAAACCCCT-3′
		5′-ACACAGGCCTTTGTTGTTGT-3′
gelsolin	270	5′-TGTGATCGAAGAGGTTCCTG-3′
		5′-GACCAGTAATCATCATCCCA-3′
β-actin	51	5′-AGGCACCAGGGCGTGAT-3′
		5′-GCCCACATAGGAATCCTTCTGAC-3′
GAPDH	414	5′-CATGGAGGAGGCTGGGGCTC-3′
		5′-CACTGACACGTTGGCAGTGG-3′

Scientific, San Jose, CA, USA). The following parameters for dynamic exclusion were applied: 1 repeat count, 30 ms repeat duration, 500 exclusion list size, 120 s exclusion duration, exclusion width low energy 0.51; exclusion width high energy 1.51. The peptides identified in all LC−MS/MS analyses were merged into a common list, which was next overlaid onto 2-D maps generated from the LC/MS profile data of individual samples, as previously reported.[23]

Bioinformatic Analysis. The acquired raw data were processed to produce peak lists by Mascot Distiller software (version 2.2.1, Matrix Science, London, UK). The resulting ion lists were searched using the Mascot search engine (version 2.2.03, Matrix Science) against a database comprising all human protein entries from the Sprot and their reversed versions. The search parameters were as follows: enzyme specificity, trypsin; variable modifications, oxidation (M); and protein mass, unrestricted. The peptide and fragment ion mass tolerances used were 20 ppm and 0.6 Da, respectively. Peptides with Mascot score exceeding the threshold value corresponding to <5% false positive rate calculated by Mascot procedure were considered to be positively identified. At least two peptides for each protein with a score above the threshold were required for the identification. The qualitative analysis of protein/peptide lists generated by the Mascot search engine was performed using MScan, whereas for quantitative estimation the MSparky software tool was used. The statistical analysis was performed using the DiffProt software, thereby obtaining a list of differentially expressed proteins. For each of them the R (ratio) and F (fold change) values were estimated to identify up-/down-regulation and fold changing, respectively. Data are shown as mean ± s.e.m. of independent triplicate experiments. The p values obtained were corrected for multiple-hypothesis testing using a two-step Benjamini−Hochberg procedure that controlled for the false discovery rate.[23] The relative protein abundances with adjusted p values ≤ 0.05 and fold-change (FC) values ≥ 1.5 were considered as significant in at least one of the studied groups. For graphical summaries and to evaluate the relationships among the studied samples, we used principal component analysis and Ward's linkage hierarchical clustering. All statistical analyses were performed with MStat software. The software used for bioinformatics analyses were available at http://proteom.ibb.waw.pl/index.en.html.

Comet Assay. The extent of DNA damage in individual cells was established by single cell gel electrophoresis using the OxiSelect Comet assay kit (Cell Biolabs, San Diego, CA, USA) according to the manufacturer's instructions. Briefly, 1 × 105 MDA-MB231 cells were seeded in 75 cm^2 flasks in control conditions or treated with either 8.45 μM JAHA, 2.5 μM etoposide (VP16), or a mixture of the two compounds, for 48 h. At the end of incubation, mechanically detached cells were centrifuged, washed, and resuspended at 1 × 105/mL concentration in Ca^{++}/Mg^{++}-free PBS at 4 °C. The samples were mixed with Comet agarose (1:10 ratio, v/v) and the mixture spread onto the OxiSelect Comet slides and allowed to gel. The slides were then incubated with lysis buffer (4 °C, 45 min in the dark) followed by treatment with an alkaline solution (4 °C, 30 min in the dark) to allow DNA relaxation and denaturation. The damaged DNA was separated by the intact fraction by alkaline gel electrophoresis in an horizontal chamber (15 V, 30 min) in TBE running buffer to detect both single-stranded and double-stranded DNA breaks. At the end of the run, the slides were immersed in cold 70% ethanol for 5 min, air-dried, stained with Vista Green DNA Dye, observed with a Nikon Microphot SA fluorescence microscope, and image analysis performed with CASP Version 1.2.3b1 software (Sourceforge, Diceholdings Inc., New York, NY, USA). Samples were run in triplicate and cells were selected randomly for the analysis per slide. DNA damage was estimated on the basis of tail length (TL), tail moment (TM), olive tail moment (OTM), and % tail DNA (% DNA). Statistical analysis of the data was performed using Excel software.

RESULTS

To search for differentially expressed genes in MDA-MB231 cells exposed to 8.45 μM HDACis for 18, 24, and 48 h, DD-PCR was performed on enriched mRNA samples isolated from control and treated cell preparations, in the presence of combinations of the arbitrary primers, as listed previously. After PAGE and silver stain, a number of bands appeared differently displayed in parallel control and treated samples, and they were cut from the gel and submitted to further analysis. To this

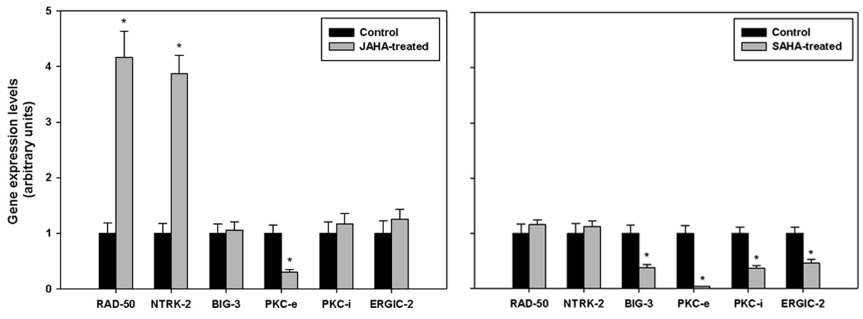

Figure 1. Quantitative real-time PCR analysis of the transcript levels of RAD-50, NTRK2, BIG-3, PKCε, PKCι, and ERGIC-2 in MDA-MB231 cells exposed to either 8.45 μM (A) JAHA or (B) SAHA for 24 h (RAD-50 and NTRK2) or 48 h (BIG-3, PKCε, PKCι, and ERGIC-2). Beta-actin was used as an internal control. Values are the mean ± s.e.m. of two quadruplicate experiments. ∗ indicates $p < 0.01$ (student's t test).

DOI: 10.1021/acs.chemrestox.7b00269
Chem. Res. Toxicol. 2017, 30, 2187−2196

purpose, the cDNA contained in the bands was purified, reamplified until purity and adequate yield, and then the material was submitted to sequencing. Following BLAST analysis, homology was found between six DD-bands and portions of cDNAs of the following genes: (i) Neurotrophic tyrosine kinase, receptor, type 2 (NTRK-2 a.k.a. TRKB, NM_001018064.1), and (ii) RAD50 DNA repair protein (NM_005732.3) both in 24 h-exposure preparations; (iii) Brefeldine A-inhibited guanine nucleotide-exchange protein 3 (BIG-3, NM_020340.3), (iv) Protein kinase C epsilon (PKCε, NM_005400.2), (v) Protein kinase C iota (PKCι; NM_002740.5), (vi) Endoplasmic reticulum−Golgi intermediate compartment 2KDa protein (ERGIC-2, NM_016570.2), all in 48 h exposure preparations.

Real time PCR assays were carried out to validate the DD-PCR data since it is known that the technique may give false positive results; in addition, to confirm the specificity of the HDACi-linked gene signatures, the expression of the genes differentially displayed in case of either conditions of exposure was cross-checked also in parallel control- and treated cell preparations obtained after exposure to the other inhibitor. As shown in Figure 1, JAHA at 8.45 μM concentration prominently induced the expression of *RAD50* and *NTRK-2* genes after 24 h of treatment, while it reduced the expression of *PKC*ε after 48 h of treatment; on the other hand, the data obtained with SAHA at the same concentration show a clear reduction in the expression levels of *BIG-3*, *PKC*ι, and *ERGIC-2* genes after 48 h of treatment. Noteworthy, the cross-check test demonstrated a drastic down-regulation of *PKC*ε also in MDA-MB231 cells treated for 48 h with SAHA. No significant change was found in the expression levels of *RAD50* and *NTRK2* in SAHA-exposed cells and of *BIG-3*, *PKC*ι, and *ERGIC-2* in JAHA-exposed cells.

Previous literature data[4] reported that SAHA-exposed MDA-MB231 cells developed up-regulation of some genes associated with differentiation and/or growth inhibition, that is, those encoding for gelsolin, isopentenyl-diphosphate delta isomerase-1 (IDI1), and 1,25-dihydroxyvitamin D-3 up-regulated protein-1 (VDUP1). To extend the comparative evaluation of the molecular effects of SAHA and JAHA inhibitors on MDA-MB231 cells, we checked by real time PCR the effects of MDA-MB231 cell treatment with 8.45 μM JAHA for 48 h on the expression levels of the same genes identified as up-regulated in SAHA-treated cells. The results obtained show a similarity of action of SAHA and JAHA on the expression levels of the genes examined (Figure 2).

To expand the search of JAHA-associated signatures at the protein level, proteomic analyses were performed and showed a differential expression of 11 proteins (six, one, and four associated to 18, 24, and 48 h of treatment with JAHA at 8.45 μM, respectively). As shown in Table 2, of the six proteins associated to 18 h-treatment, four were down-regulated (i.e., Neuroblast differentiation-associated protein AHNAK protein, High mobility group protein B2, Cystatin-B, High mobility group protein B1) and two were up-regulated (i.e., Ribosome-binding protein 1, Glutaredoxin-1) in treated samples. A single up-regulated protein (i.e., Hematological and neurological expressed 1 protein a.k.a. HN1) was found in cells treated with JAHA for 24 h, and four up-regulated proteins in cells treated with JAHA for 48 h (i.e., Prelamin-A/C, Ribosome-binding protein 1, Sulfiredoxin-1, Histone H1.0).

Twenty-two proteins appeared to be differentially expressed in cells treated with SAHA at the same concentration (16, 5, and 1, respectively, associated to 18, 24, and 48 h-treatment). Of the 16 proteins identified at 18 h-treatment, six were down-regulated (i.e., Reticulocalbin-1, Microtubule-associated protein 1B, Caprin-1, Spectrin α chain nonerythrocytic 1, Integrin β1, Myristoylated alanine-rich C-kinase substrate), whereas the other ones were up-regulated in the treated samples (i.e., Histone H1.0, Neuroblast differentiation-associated protein AHNAK, Hematological and neurological expressed protein 1 a.k.a. HN1, Nucleolar and coiled-body phosphoprotein 1, Nucleolin, Eukaryotic translation initiation factor 4H, 78 kDa Glucose-regulated protein, Histidine triad nucleotide-binding protein 2 mitochondrial, Na+/H+ exchange regulatory cofactor NHE-RF1, Nonerythrocytic spectrin alpha chain 1, Integrin β1, Heterogeneous nuclear ribonucleoproteins A2/B1). Of the five proteins associated to 24 h-treatment, two were down-regulated (i.e., Neuroblast differentiation-associated protein AHNAK, Nicotinamide phosphoribosyltransferase) and three were up-regulated (i.e., Na+/H+ exchange regulatory cofactor NHE-RF1, Histone H1, 78 kDa Glucose-regulated protein). Finally, a single protein was identified as down-regulated (Neuroblast differentiation-associated protein AHNAK) in the samples treated with the inhibitor for 48 h (Table 3).

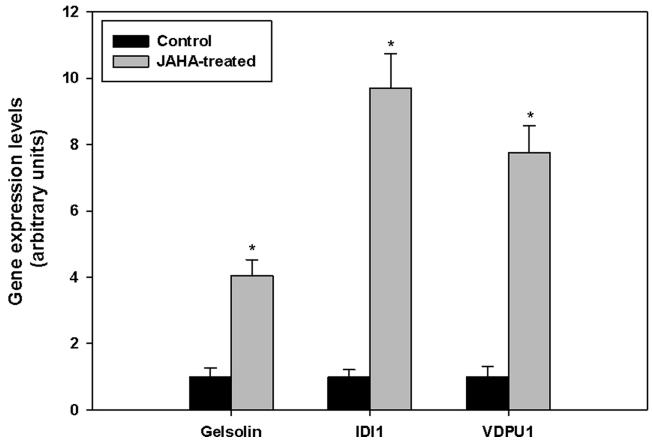

Figure 2. Quantitative real-time PCR analysis of the transcript levels of gelsolin, IDI1, and VDPU1 in MDA-MB231 cells exposed to 8.45 μM JAHA for 48 h. Beta-actin was used as an internal control. Values are the mean ± s.e.m. of two quadruplicate experiments. ∗ indicates $p < 0.01$ (student's t test).

The finding that exposure to JAHA induced the selective up-regulation of molecular signatures linked to the processes of DNA repair and response to oxidative stress, such as *NTRK-2*, *RAD50*, sulfiredoxin-1, and glutaredoxin-1, prompted to check the related "in cellulo" effect by examining whether the presence of this HDACi could reverse the production of DNA lesions induced by the topoisomerase IIα inhibitor VP16. The genotoxic effect of JAHA was assessed in MDA-MB231 breast cancer cells using Comet assay. The panel in Figure 3 show the very low level of DNA damage in control and 8.45 μM JAHA-treated cells in contrast to 2.5 μM VP16-treated cells, as shown by the mean DNA tail moment indicative of persistent double- and single-strand breaks. Interestingly, DNA damage induced by the latter was reduced by 50% when cells were coexposed to 8.45 μM JAHA and 2.5 μM VP16, as displayed by the decrease of the DNA tail moment. Although, as compared to the basal level of control cells, the total DNA damage appeared not to be entirely reversible by VP16/JAHA cotreatment, nevertheless this result confirms that the DNA repair system was efficiently switched-on in the presence of the HDACi, as suggested by

DOI: 10.1021/acs.chemrestox.7b00269
Chem. Res. Toxicol. 2017, 30, 2187−2196

Table 2. Differentially-Expressed Proteins Identified in MDA-MB231 Cells Cultured in Control Conditions and Exposed to 8.45 μM JAHA for 18, 24, and 48 h

accession no.	protein	Q value	ratio (control/treated)	fold change	peptides
18 h					
Q09666	Neuroblast differentiation-associated protein AHNAK	0.00079	1.35	1.35	276
P26583	High mobility group protein B2	0.00158	2.44	2.44	12
P04080	Cystatin-B (a.k.a Stefin-B)	0.02422	2.94	2.94	7
Q9P2E9	Ribosome-binding protein 1 (RRBP1)	0.02587	0.61	1.64	22
P09429	High mobility group protein B1	0.08112	2.70	2.70	11
P35754	Glutaredoxin-1	0.08978	0.48	2.09	5
24 h					
Q9UK76	Hematological and neurological expressed 1 protein (HN1)	0.02226	0.44	2.26	10
48 h					
P02545	Prelamin-A/C	0.00075	0.5	2.00	36
Q9P2E9	Ribosome-binding protein 1 (RRBP1)	0.01057	0.42	2.36	24
Q9BYN0	Sulfiredoxin-1	0.04155	0.12	8.55	3
P07305	Histone H1.0	0.04578	0.20	5.05	6

Table 3. Differentially-Expressed Proteins Identified in MDA-MB231 Cells Cultured in Control Conditions and Exposed to 8.45 μM SAHA for 18, 24, and 48 h

accession no.	protein	Q value	ratio (control/treated)	fold change	peptides
18h					
P07305	Histone H1.0	0.00035	0.11	9.03	6
Q09666	Neuroblast differentiation-associated protein AHNAK	0.00035	1.41	1.41	257
Q9UK76	Hematological and neurological expressed 1 protein (HN1)	0.00280	0.47	2.13	10
Q15293	Reticulocalbin-1	0.00469	2.60	2.60	13
Q14978	Nucleolar and coiled-body phosphoprotein 1	0.00489	0.54	1.85	17
P19338	Nucleolin	0.00545	0.51	1.96	28
Q15056	Eukaryotic translation initiation factor 4H	0.00559	0.49	2.04	7
P46821	Microtubule-associated protein 1B	0.01389	2.03	2.03	14
Q14444	Caprin-1	0.01565	1.75	1.75	11
P11021	78 kDa glucose-regulated protein	0.01623	0.64	1.56	35
Q9BX68	Histidine triad nucleotide-binding protein 2, mitochondrial	0.01679	0.20	4.97	3
O14745	Na(+)/H(+) exchange regulatory cofactor NHE-RF1	0.01776	0.37	2.71	4
Q13813	Spectrin alpha chain, nonerythrocytic 1	0.01849	1.51	1.51	36
P05556	Integrin β1	0.01877	1.67	1.67	10
P22626	Heterogeneous nuclear ribonucleoproteins A2/B1	0.02038	0.55	1.81	14
P29966	Myristoylated alanine-rich C-kinase substrate	0.05348	1.98	1.98	10
24 h					
Q09666	Neuroblast differentiation-associated protein AHNAK	0.00072	1.53	1.53	267
O14745	Na^+/H^+ exchange regulatory cofactor NHE-RF1	0.00502	0.26	3.79	4
P07305	Histone H1.0	0.01815	0.54	1.85	6
P11021	78 kDa glucose-regulated protein	0.03586	0.55	1.83	35
P43490	Nicotinamide phosphoribosyltransferase	0.05941	3.04	3.04	9
48 h					
Q09666	Neuroblast differentiation-associated protein AHNAK	0.08576	2.26	2.26	254

some of the revealed molecular signatures associated with exposure of MDA-MB231 breast cancer cells to JAHA.

DISCUSSION

Breast tumor is a widely spread neoplastic histotype accounting for about 20% of all cancers in women; about 15% of breast cancers are TNBC and the lack of receptors for estrogens, progesterone, and epidermal growth factor renders neoplastic cells highly aggressive and endowed with a higher malignant potential than other breast tumor subtypes (e.g., ref 24). Since the pharmacological options for treating TNBC are limited, there has been great interest in testing novel drugs or analogues of pre-existing drugs counteracting TNBC cell growth, which, on the other hand, necessitates a comprehensive biological characterization. The effects of the HDACi JAHA on aspects of the biology of TNBC MDA-MB231 cells, such as survival, cell cycle, mitochondrial activity, autophagy, apoptosis, and signal transduction, have been the object of previous publications.[16,25] Since it is widely acknowledged that multiplatform classification of breast cancers is based on genomic sequencing, gene expression profiling, and proteomics, the present study was focused on the evaluation of some molecular aspects of the effects exerted by JAHA on this cell line, also comparing with those related to exposure to the parental HDACi SAHA.

For this reason, to supplement the catalogue of JAHA- (and in parallel SAHA-) dependent genes and search for putative molecular markers linked to the lethal action of JAHA, cDNA samples obtained from enriched mRNA preparations of MDA-

DOI: 10.1021/acs.chemrestox.7b00269
Chem. Res. Toxicol. 2017, 30, 2187−2196

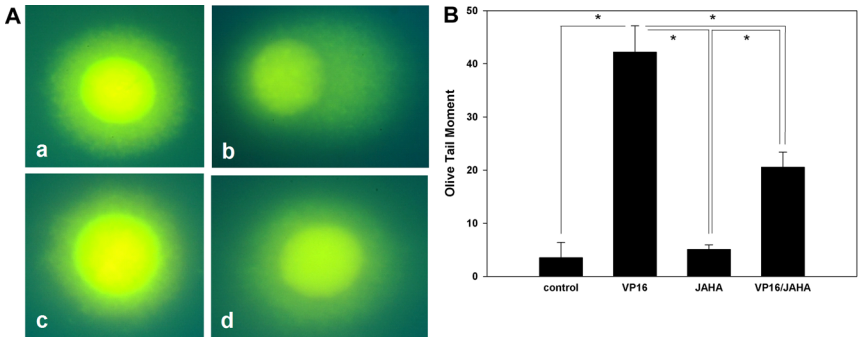

Figure 3. (A) Representative micrographs of cell comets obtained from MDA-MB231 TNBC cells stained with Vista Green DNA Dye, observed with a Nikon Microphot SA fluorescence microscope: (a) control cells, (b) cells treated with 2.5 μM VP16 for 48 h, (c) cells treated with 8.45 μM JAHA for 48 h, and (d) cells cotreated with 8.45 μM JAHA and 2.5 μM VP16 for 48 h. Microscopic magnification = 400×. (B) Histograms showing the olive tail moment of the scored cells exposed to VP16, JAHA, and VP16/JAHA, as compared to control (n = 60 for each experimental condition). Values are the mean ± s.e.m. of the results obtained. ∗ indicates $p < 0.05$ (student's t test).

MB231 cells, both control and treated with the HDACis, were submitted to DD-PCR assay and the results obtained were confirmed by real time-PCR assay. In parallel, protein extracts from control and exposed cells were comparatively studied via mass spectrometry and bioinformatics. The results obtained indicate that under the same experimental conditions JAHA and SAHA, although sharing some common aspects, induce a diversified molecular reprogramming and allow one to draw the following conclusions.

Exposure of cells to JAHA appeared to selectively trigger an early and approximately four-fold overexpression of two oxidative-stress related genes, that is, *NTRK-2* and *RAD-50*. The former encodes for a member of the tropomyosin-related kinase family of neurotrophin receptors, which is up-regulated in several human cancers, including TNBC, where it was found to be involved in epithelial-mesenchymal transition, anoikis resistance, and metastatic spread.[26,27] In addition, a number of studies performed on nerve and choriocarcinoma cell models have demonstrated its powerful role in repair of oxidative DNA damage and related inhibition of apoptosis. In particular, in rat cortical neurons the NTRK-2 protective activity was found to be accomplished via PI3K, pAKT, pCREB, and the expression of *APE1* (apurinic/apyrimidinic endonuclease-1), a key component of the base excision DNA repair pathway.[28,29] RAD-50 is known to participate with MRE11 and NBS1 to the formation of the MRN complex, which coordinates the repair of DNA double strand breaks in the nucleus.[30] The inability of SAHA to trigger RAD50 up-regulation was demonstrated also in prostate cancer cells by Lee et al.,[31] thereby further confirming that this is a JAHA-selective gene signature. Evidence of JAHA's role as antioxidative stress compound emerged also from proteomic analyses demonstrating the specific accumulation of glutaredoxin-1, cystatin-B, and, more prominently and at a later time, sulfiredoxin-1. The latter one is an ATP-dependent cytoprotective antioxidant enzyme known to catalyze peroxiredoxin reactivation and deglutathionylation of glutathionylated proteins in several cytotypes exposed to diversified chemical and biological stimuli that elicit the production of reactive oxygen species.[32] Glutaredoxin-1 catalyzes the reversible reduction of glutathione-protein mixed disulfides and is implicated in DNA repair and mitochondrial DNA synthesis, thereby highly contributing to the antioxidant cellular defense system.[33] Cystatin-B is an inhibitor of lysosomal cysteine cathepsin that has been proven to protect mouse mammary tumor cells from oxidative stress and consequent death.[34] The ability of JAHA to reverse DNA damage in cultured cells, at least in part, was demonstrated by a Comet assay in JAHA/VP16 cotreatment experiments thereby further substantiating that there is a correlation between the increase of the molecular signatures involved in DNA repair mechanisms and the peculiar ability of JAHA to reduce DNA damage, through a molecular mechanism, which is still to be determined. Noteworthy, this finding is contrary to what has been described as a general aspect of HDACis,[35] that is, the inhibition of different aspects of DNA repair including the interference with coordination of ataxia-telangiectasia and Rad3-related (ATR) activation and signaling, which is downstream Rad50 phosphorylation;[36] this peculiar property of JAHA seems truly interesting since it is uncommon but beneficial to find a HDACi that simultaneously increases DNA repair. Other specific JAHA signatures are represented by the early down-regulation of the high mobility group proteins and the up-regulation of RRBP1 that continues also in later time coupled with the late up-regulation of prelamin A/C. The first ones are architectural transcription factors, and a miRNA-triggered decrease of the amount of high mobility group protein-B1 has been proven to impair MDA-MB231 cell cycle progression and render these and other mammalian cytotypes sensitive to a number of diversified death stimuli.[37,38] Noteworthy, high mobility group proteins-B1 and -B2 are known to play a DNA damage-sensing role and induce phosphorylation of p53 as a response;[39] therefore, the decrease of the intracellular amount of these chromatin-associated factors may be responsible, at least in part, of the previously observed lack of apoptosis induction after cell exposure to JAHA.[25] On the other hand, apoptosis restraining could also result from constant RRBP1 accumulation; this ribosome-binding factor is associated with unfolded protein response in the endoplasmic reticulum and its up-regulation has been found to render lung cancer cells more resistant to the stress and to alleviate apoptosis.[40] Accumulation of prelamin A-C is indicative of impairment of protein farnesylation which is a prerequisite for its processing.[41] It is known that farnesylated species are cytotoxic, and in particular the accumulation of prelamin A in fibroblasts by siRNA transfection has been shown to increase the levels of reactive oxygen species, affect mitochondrial respiration, and alter the expression of the genes encoding detoxifying enzymes.[42] In addition, it is worth mentioning that farnesylation represents a maturation step for Ras GTPase,[43] and therefore, if JAHA determines in some way

DOI: 10.1021/acs.chemrestox.7b00269
Chem. Res. Toxicol. 2017, 30, 2187−2196

the inhibition of farnesyltransferase activity as suggested by accumulation of prelamin, it may exert its lethal effect by also targeting other substrates that play pivotal roles in the control of cell survival and growth.

A number of molecular signatures were shared between JAHA and SAHA. DD-PCR experiments demonstrated that the two HDACis were able to induce a late PKCε down-regulation. It is known that the down-regulation of this protein in MDA-MB231 cells accounts for a reduced transcriptional activity of NF-κB due to a significant inhibition of nuclear translocation of p65. This may lead to the alteration of the expression of genes involved in cell survival and proliferation,[44] which may be one of the aspects involved in the already-observed perturbation of MDA-MB231 cell cycle by JAHA,[25] and expands the list of shared gene signatures associated with differentiation or growth inhibition, such as gelsolin, IDI1, and VDUP1. From proteomic analyses, it appeared that JAHA and SAHA shared also a decrease of the amount of the neuroblast differentiation-associated protein AHNAK, more prolonged in the presence of SAHA, and the increase of the amount of histone H1.0, earlier in the presence of SAHA, and of HN1. Also histone H1.0 and HN1 represent growth-associated factors. It is already known that *histone H1.0* gene expression is sensitive to the state of chromatin acetylation, and in particular to the inhibition of HDAc, as found for trichostatin A-treated mouse mammary tumor cells.[45] An immunohistochemical study on breast cancer specimens of different histological grading has strongly suggested that *histone H1.0* expression is linked to a prolongation of cell intermitotic period irrespective of cell malignant potential, thereby representing a marker of a low proliferative activity.[46] On the other hand, HN1, which is an interaction partner of the inactive GSK3β/β-catenin/APC complex contributing to ubiquitin-dependent proteasomal degradation of β-catenin, when overexpressed in prostate cancer cells have been shown to trigger their accumulation at G_2/M checkpoint, and to reduce the proliferation rate.[47] These literature data are consistent with our previous results[25] demonstrating cell cycle perturbation and a delay in G_2/M transition in MDA-MB231 cells exposed to JAHA. Various are the intracellular roles played by the giant AHNAK protein in very diverse biological processes.[48] In breast cancer, this protein was found to be localized in lipid rafts thus suggesting its involvement in signaling pathways also linked with the reorganization of actin submembraneous network.[49] In particular, when AHNAK was overexpressed in TNBC cell lines, such as MDA-MB231, a marked inhibition of ERK phosphorylation was observed; therefore, it is conceivable that JAHA-mediated AHNAK down-regulation in this cell line may be at least in part responsible of the observed early reduction of the amount of pERK in MDA-MB231 wells exposed to JAHA, as reported by Librizzi et al.[16]

A number of genes and, more prominently, protein signatures, involved in different biological events have been found associated only to SAHA-, and not JAHA-, treatment under the same experimental conditions. Thus, as opposed to SAHA, JAHA did not appear to be active on the control of specific enzyme activities via (i) the down-regulation of the expression of *BIG-3* encoding for an A-kinase anchoring protein,[50] and of *PKCι* whose depletion have been proven to restrain TNBC growth and address cells to senescence,[51,52] (ii) the increase of accumulation of eukaryotic translation initiation factor 4H, an activator of the RNA helicase eIF4A,[53] and (iii) the decrease of the amount of nicotinamide phosphoribosyltransferase, whose inhibition was found to suppress breast tumor growth *in vivo* in a xenograft model.[54] Other biological mediators whose expression/accumulation was affected by SAHA, but not JAHA, are (i) the proliferation- and cell cycle-affecting factors ERGIC-2,[55] myristoylated alanine-rich C-kinase substrate,[56] nucleolin,[57] nucleolar and coiled-body phosphoprotein 1,[58] reticulocalbin-1,[59] spectrin alpha chain, nonerythrocytic 1,[60] and caprin-1,[61] (ii) the autophagy marker microtubule-associated protein 1B,[62] (iii) the endoplasmic reticulum chaperone 78 kDa glucose-regulated protein,[63] and (iv) signaling molecules such as the extracellular matrix receptor subunit integrin β1,[64] the ERK-activating factor heterogeneous nuclear ribonucleoproteins A2/B1,[65] the EGFR regulator Na(+)/H(+) exchange regulatory cofactor NHE-RF1,[66] and the inhibitor of Wnt/β-catenin pathway histidine triad nucleotide-binding protein 2.[67]

In summary, in this study we have established a number of molecular signatures in response to the HDACi JAHA in a TNBC cell model, and although this compound is closely related to the parental molecule SAHA, we have revealed some substantial differences in the biomarkers of drug responses. In contrast to the more numerous and diversified changes induced by SAHA, JAHA displays a more selective impact on the expression of molecular signatures by increasing the expression of some molecular signatures involved in antioxidant activity and DNA repair. This specific property will represent a challenge, which must be taken into account in a future consideration of this molecule as an anticancer drug. Literature data have already reported the effect of SAHA or other HDACis on only five among the molecular signatures identified in this study, that is, 78 kDa glucose-regulated protein, integrin β1, NHE-RF1, reticulocalbin-1, and histone H1.0.[68−72] Therefore, our work also contributes to expand the list of molecular signature responsive to cell exposure to these enzyme inhibitors. On the basis of the present exploratory study, further work using global gene expression and proteomic profiling protocols will allow a further understanding of the selective molecular response associated with their mechanisms of action, and to define key client transcripts and proteins for either specific compound with potential clinical significance minimizing the problematic effects and emphasizing the therapeutic ones.

AUTHOR INFORMATION

Corresponding Author

*E-mail: fabio.caradonna@unipa.it. Phone: +3909123897331.

ORCID

Fabio Caradonna: 0000-0002-7659-7312
Michał Dadlez: 0000-0002-8749-9224
John Spencer: 0000-0001-5231-8836
Claudio Luparello: 0000-0001-9821-5891

Author Contributions

The manuscript was written through contributions of all authors. All authors have given approval to the final version of the manuscript.

Funding

Work was partly funded by University of Palermo/Italy (FFR 2013), the Italian Ministero dell'Istruzione, dell'Università e della Ricerca (MIUR) (PON 01_01059.) to C.L. and M.L., and the Royal Thai Government to S.S.

Notes

The authors declare no competing financial interest.

DOI: 10.1021/acs.chemrestox.7b00269
Chem. Res. Toxicol. 2017, 30, 2187−2196

ABBREVIATIONS

HDACi, histone deacetylase inhibitor; SAHA, suberoylanilide hydroxamic acid; TNBC, triple-negative breast cancer; JAHA, Jay Amin hydroxamic acid; IC_{50}, half maximal inhibitory concentration; pERK, phosphorylated extracellular signal-related kinase; DNMT, DNA methyltransferase; PCR, polymerase chain reaction; EDTA, ethylenediaminetetraacetic acid; DD, differential display; PAGE, polyacrylamide gel electrophoresis; dNTP, deoxynucleotide triphosphate; GAPDH, glyceraldehyde 3-phosphate dehydrogenase; EGTA, ethylene-bis (oxyethylenenitrilo) tetraacetic acid; SDS, sodium dodecyl sulfate; BCA, bicinchoninic acid; HPLC, high performance liquid chromatography; LC−MS/MS, liquid chromatography−tandem mass spectrometry; s.e.m., standard error of the mean; NTRK-2, neurotrophic tyrosine kinase, receptor, type 2; BIG-3, brefeldine A-inhibited guanine nucleotide-exchange protein 3; PKCε, protein kinase C epsilon; PKCι, protein kinase C iota; ERGIC-2, endoplasmic reticulum-Golgi intermediate compartment 2KDa protein; IDI1, isopentenyl-diphosphate delta isomerase-1; VDUP1, 1,25-dihydroxyvitamin D-3 up-regulated protein-1; RRBP1, ribosome-binding protein 1; HN1, hematological and neurological expressed 1 protein; NHE-RF1, Na(+)/H(+) exchange regulatory cofactor; PI3K, phosphatidylinositol-4,5-bisphosphate 3-kinase; pCREB, phosphorylated cyclic AMP response element binding; APE1, apurinic/apyrimidinic endonuclease-1; MRN, Mre11-Rad50-Nbs1; siRNA, short interfering RNA; GSK3β, glycogen synthase kinase 3 beta; APC, adenomatous polyposis coli; EGFR, epidermal growth factor receptor; ATR, ataxia-telangiectasia and Rad3-related

REFERENCES

(1) Mottamal, M., Zheng, S., Huang, T. L., and Wang, G. (2015) Histone deacetylase inhibitors in clinical studies as templates for new anticancer agents. *Molecules 20*, 3898−3941.

(2) Mann, B. S., Johnson, J. R., Cohen, M. H., Justice, R., and Pazdur, R. (2007) FDA approval summary: vorinostat for treatment of advanced primary cutaneous T-cell lymphoma. *Oncologist 12*, 1247−1252.

(3) Shastry, M., and Yardley, D. A. (2013) Updates in the treatment of basal/triple-negative breast cancer. *Curr. Opin. Obstet. Gynecol. 25*, 40−48.

(4) Huang, L., and Pardee, A. B. (2000) Suberoylanilide hydroxamic acid as a potential therapeutic agent for human breast cancer treatment. *Mol. Med. 6*, 849−866.

(5) Zhou, Q., Shaw, P. G., and Davidson, N. E. (2009) Inhibition of histone deacetylase suppresses EGF signaling pathways by destabilizing EGFR mRNA in ER-negative human breast cancer cells. *Breast Cancer Res. Treat. 117*, 443−451.

(6) Librizzi, M., Spencer, J., and Luparello, C. (2016) Biological effect of a hybrid anticancer agent based on kinase and histone deacetylase inhibitors on triple-negative (MDA-MB231) breast cancer cells. *Int. J. Mol. Sci. 17*, E1235.

(7) Feng, X., Han, H., Zou, D., Zhou, J., and Zhou, W. (2017) Suberoylanilide hydroxamic acid-induced specific epigenetic regulation controls leptin-induced proliferation of breast cancer cell lines. *Oncotarget 8*, 3364−3379.

(8) Kim, S. A., Jin, Y. L., and Kim, H. S. (2009) Structure-activity relationship studies of novel oxygen-incorporated SAHA analogues. *Arch. Pharmacal Res. 32*, 15−21.

(9) Spencer, J., Amin, J., Wang, M., Packham, G., Alwi, S. S., Tizzard, G. J., Coles, S. J., Paranal, R. M., Bradner, J. E., and Heightman, T. D. (2011) Synthesis and biological evaluation of JAHAs: ferrocene-based histone deacetylase inhibitors. *ACS Med. Chem. Lett. 2*, 358−362.

(10) Marzenell, P., Hagen, H., Sellner, L., Zenz, T., Grinyte, R., Pavlov, V., Daum, S., and Mokhir, A. (2013) Aminoferrocene-based prodrugs and their effects on human normal and cancer cells as well as bacterial cells. *J. Med. Chem. 56*, 6935−6944.

(11) Jaouen, G., Vessières, A., and Top, S. (2015) Ferrocifen type anti cancer drugs. *Chem. Soc. Rev. 44*, 8802−8817.

(12) Leonidova, A., Anstaett, P., Pierroz, V., Mari, C., Spingler, B., Ferrari, S., and Gasser, G. (2015) Induction of cytotoxicity through photorelease of aminoferrocene. *Inorg. Chem. 54*, 9740−9748.

(13) Patra, M., and Gasser, G. (2017) The medicinal chemistry of ferrocene and its derivatives. *Nat. Rev. Chem. 1*, 0066.

(14) Ocasio, C. A., Sansook, S., Jones, R., Roberts, J. M., Scott, T. G., Tsoureas, N., Coxhead, P., Guille, M., Tizzard, G. J., Coles, S. J., Hochegger, H., Bradner, J. E., and Spencer, J. (2017) *Organometallics 36*, 3276−3283.

(15) Li, J., Liu, R., Lei, Y., Wang, K., Lau, Q. C., Xie, N., Zhou, S., Nie, C., Chen, L., Wei, Y., and Huang, C. (2010) Proteomic analysis revealed association of aberrant ROS signaling with suberoylanilide hydroxamic acid-induced autophagy in Jurkat T-leukemia cells. *Autophagy 6*, 711−724.

(16) Librizzi, M., Chiarelli, R., Bosco, L., Sansook, S., Gascon, J. M., Spencer, J., Caradonna, F., and Luparello, C. (2015) The histone deacetylase inhibitor JAHA down-regulates pERK and global DNA methylation in MDA-MB231 breast cancer cells. *Materials 8*, 7041−7047.

(17) Sirchia, R., and Luparello, C. (2009) Short-term exposure to cadmium affects the expression of stress response and apoptosis-related genes in immortalized epithelial cells from the human breast. *Toxicol. In Vitro 23*, 943−949.

(18) Luparello, C., Longo, A., and Vetrano, M. (2012) Exposure to cadmium chloride influences astrocyte-elevated gene-1 (AEG-1) expression in MDA-MB231 human breast cancer cells. *Biochimie 94*, 207−213.

(19) Luparello, C., Sirchia, R., and Longo, A. (2013) Type V collagen and protein kinase C η down-regulation in 8701-BC breast cancer cells. *Mol. Carcinog. 52*, 348−358.

(20) Sokolov, B. P., and Prockop, D. J. (1994) A rapid and simple PCR-based method for isolation of cDNAs from differentially expressed genes. *Nucleic Acids Res. 22*, 4009−4015.

(21) Naselli, F., Belshaw, N. J., Gentile, C., Tutone, M., Tesoriere, L., Livrea, M. A., and Caradonna, F. (2015) Phytochemical indicaxanthin inhibits colon cancer cell growth and affects the DNA methylation status by influencing epigenetically modifying enzyme expression and activity. *J. Nutrigenet. Nutrigenomics 8*, 114−127.

(22) Rozek, W., Kwasnik, M., Debski, J., and Zmudzinski, J. F. (2013) Mass spectrometry identification of granins and other proteins secreted by neuroblastoma cells. *Tumor Biol. 34*, 1773−1781.

(23) Bakun, M., Senatorski, G., Rubel, T., Lukasik, A., Zielenkiewicz, P., Dadlez, M., and Paczek, L. (2014) Urine proteomes of healthy aging humans reveal extracellular matrix (ECM) alterations and immune system dysfunction. *Age (Dordr.) 36*, 299−311.

(24) Gluz, O., Liedtke, C., Gottschalk, N., Pusztai, L., Nitz, U., and Harbeck, N. (2009) Triple-negative breast cancer - current status and future directions. *Ann. Oncol. 20*, 1913−1927.

(25) Librizzi, M., Longo, A., Chiarelli, R., Amin, J., Spencer, J., and Luparello, C. (2012) Cytotoxic effects of Jay Amin hydroxamic acid (JAHA), a ferrocene-based class I histone deacetylase inhibitor, on triple-negative MDA-MB231 breast cancer cells. *Chem. Res. Toxicol. 25*, 2608−2616.

(26) Howe, E. N., Cochrane, D. R., and Richer, J. K. (2011) Targets of miR-200c mediate suppression of cell motility and anoikis resistance. *Breast Cancer Res. 13*, R45.

(27) Kim, M. S., Lee, W. S., Jeong, J., Kim, S. J., and Jin, W. (2015) Induction of metastatic potential by TrkB via activation of IL6/JAK2/STAT3 and PI3K/AKT signaling in breast cancer. *Oncotarget 6*, 40158−40171.

(28) Fujita, K., Tatsumi, K., Kondoh, E., Chigusa, Y., Mogami, H., Fujii, T., Yura, S., Kakui, K., and Konishi, I. (2011) Differential

DOI: 10.1021/acs.chemrestox.7b00269
Chem. Res. Toxicol. 2017, 30, 2187−2196

expression and the anti-apoptotic effect of human placental neurotrophins and their receptors. *Placenta 32*, 737−744.
(29) Yang, J. L., Lin, Y. T., Chuang, P. C., Bohr, V. A., and Mattson, M. P. (2014) BDNF and exercise enhance neuronal DNA repair by stimulating CREB-mediated production of apurinic/apyrimidinic endonuclease 1. *NeuroMol. Med. 16*, 161−174.
(30) Zhang, D., Tang, B., Xie, X., Xiao, Y. F., Yang, S. M., and Zhang, J. W. (2015) The interplay between DNA repair and autophagy in cancer therapy. *Cancer Biol. Ther. 16*, 1005−1013.
(31) Lee, J. H., Choy, M. L., Ngo, L., Foster, S. S., and Marks, P. A. (2010) Histone deacetylase inhibitor induces DNA damage, which normal but not transformed cells can repair. *Proc. Natl. Acad. Sci. U. S. A. 107*, 14639−14644.
(32) Jeong, W., Bae, S. H., Toledano, M. B., and Rhee, S. G. (2012) Role of sulfiredoxin as a regulator of peroxiredoxin function and regulation of its expression. *Free Radical Biol. Med. 53*, 447−456.
(33) Avval, F. Z., and Holmgren, A. (2009) Molecular mechanisms of thioredoxin and glutaredoxin as hydrogen donors for Mammalian s phase ribonucleotide reductase. *J. Biol. Chem. 284*, 8233−8240.
(34) Butinar, M., Prebanda, M. T., Rajković, J., Jerič, B., Stoka, V., Peters, C., Reinheckel, T., Krüger, A., Turk, V., Turk, B., and Vasiljeva, O. (2014) Stefin B deficiency reduces tumor growth via sensitization of tumor cells to oxidative stress in a breast cancer model. *Oncogene 33*, 3392−3400.
(35) Bose, P., Dai, Y., and Grant, S. (2014) Histone deacetylase inhibitor (HDACI) mechanisms of action: emerging insights. *Pharmacol. Ther. 143*, 323−336.
(36) Gatei, M., Kijas, A. W., Biard, D., Dörk, T., and Lavin, M. F. (2014) RAD50 phosphorylation promotes ATR downstream signaling and DNA restart following replication stress. *Hum. Mol. Genet. 23*, 4232−4248.
(37) Brezniceanu, M. L., Völp, K., Bösser, S., Solbach, C., Lichter, P., Joos, S., and Zörnig, M. (2003) HMGB1 inhibits cell death in yeast and mammalian cells and is abundantly expressed in human breast carcinoma. *FASEB J. 17*, 1295−1297.
(38) Chang, B. P., Wang, D. S., Xing, J. W., Yang, S. H., Chu, Q., and Yu, S. Y. (2014) miR-200c inhibits metastasis of breast cancer cells by targeting HMGB1. *J. Huazhong Univ. Sci. Technol., Med. Sci. 34*, 201−206.
(39) Krynetskaia, N. F., Phadke, M. S., Jadhav, S. H., and Krynetskiy, E. Y. (2009) Chromatin-associated proteins HMGB1/2 and PDIA3 trigger cellular response to chemotherapy-induced DNA damage. *Mol. Cancer Ther. 8*, 864−872.
(40) Tsai, H. Y., Yang, Y. F., Wu, A. T., Yang, C. J., Liu, Y. P., Jan, Y. H., Lee, C. H., Hsiao, Y. W., Yeh, C. T., Shen, C. N., Lu, P. J., Huang, M. S., and Hsiao, M. (2013) Endoplasmic reticulum ribosome-binding protein 1 (RRBP1) overexpression is frequently found in lung cancer patients and alleviates intracellular stress-induced apoptosis through the enhancement of GRP78. *Oncogene 32*, 4921−4931.
(41) Kelland, L. R., Smith, V., Valenti, M., Patterson, L., Clarke, P. A., Detre, S., End, D., Howes, A. J., Dowsett, M., Workman, P., and Johnston, S. R. (2001) Preclinical antitumor activity and pharmacodynamic studies with the farnesyl protein transferase inhibitor R115777 in human breast cancer. *Clin. Cancer Res. 7*, 3544−3550.
(42) Sieprath, T., Corne, T. D., Nooteboom, M., Grootaert, C., Rajkovic, A., Buysschaert, B., Robijns, J., Broers, J. L., Ramaekers, F. C., Koopman, W. J., Willems, P. H., and De Vos, W. H. (2015) Sustained accumulation of prelamin A and depletion of lamin A/C both cause oxidative stress and mitochondrial dysfunction but induce different cell fates. *Nucleus 6*, 236−246.
(43) Rowinsky, E. K., Windle, J. J., and Von Hoff, D. D. (1999) Ras protein farnesyltransferase: A strategic target for anticancer therapeutic development. *J. Clin. Oncol. 17*, 3631−3652.
(44) Körner, C., Keklikoglou, I., Bender, C., Wörner, A., Münstermann, E., and Wiemann, S. (2013) MicroRNA-31 sensitizes human breast cells to apoptosis by direct targeting of protein kinase C epsilon (PKC epsilon). *J. Biol. Chem. 288*, 8750−8761.
(45) Girardot, V., Rabilloud, T., Yoshida, M., Beppu, T., Lawrence, J. J., and Khochbin, S. (1994) Relationship between core histone acetylation and histone H1(0) gene activity. *Eur. J. Biochem. 224*, 885−892.
(46) Kostova, N. N., Srebreva, L. N., Milev, A. D., Bogdanova, O. G., Rundquist, I., Lindner, H. H., and Markov, D. V. (2005) Immunohistochemical demonstration of histone H1(0) in human breast carcinoma. *Histochem. Cell Biol. 124*, 435−443.
(47) Varisli, L., Gonen-Korkmaz, C., Debelec-Butuner, B., Erbaykent-Tepedelen, B., Muhammed, H. S., Bogurcu, N., Saatcioglu, F., and Korkmaz, K. S. (2011) Ubiquitously expressed hematological and neurological expressed 1 downregulates Akt-mediated GSK3β signaling, and its knockdown results in deregulated G2/M transition in prostate cells. *DNA Cell Biol. 30*, 419−429.
(48) Davis, T. A., Loos, B., and Engelbrecht, A. M. (2014) AHNAK: the giant jack of all trades. *Cell. Signalling 26*, 2683−2693.
(49) Caruso, J. A., and Stemmer, P. M. (2011) Proteomic profiling of lipid rafts in a human breast cancer model of tumorigenic progression. *Clin. Exp. Metastasis 28*, 529−540.
(50) Yoshimaru, T., Ono, M., Bando, Y., Chen, Y. A., Mizuguchi, K., Shima, H., Komatsu, M., Imoto, I., Izumi, K., Honda, J., Miyoshi, Y., Sasa, M., and Katagiri, T. (2017) A-kinase anchoring protein BIG3 coordinates oestrogen signalling in breast cancer cells. *Nat. Commun. 8*, 15427.
(51) Paget, J. A., Restall, I. J., Daneshmand, M., Mersereau, J. A., Simard, M. A., Parolin, D. A., Lavictoire, S. J., Amin, M. S., Islam, S., and Lorimer, I. A. (2012) Repression of cancer cell senescence by PKCι. *Oncogene 31*, 3584−3596.
(52) Paul, A., Gunewardena, S., Stecklein, S. R., Saha, B., Parelkar, N., Danley, M., Rajendran, G., Home, P., Ray, S., Jokar, I., Vielhauer, G. A., Jensen, R. A., Tawfik, O., and Paul, S. (2014) PKCλ/ι signaling promotes triple-negative breast cancer growth and metastasis. *Cell Death Differ. 21*, 1469−1481.
(53) Vaysse, C., Philippe, C., Martineau, Y., Quelen, C., Hieblot, C., Renaud, C., Nicaise, Y., Desquesnes, A., Pannese, M., Filleron, T., Escourrou, G., Lawson, M., Rintoul, R. C., Delisle, M. B., Pyronnet, S., Brousset, P., Prats, H., and Touriol, C. (2015) Key contribution of eIF4H-mediated translational control in tumor promotion. *Oncotarget 6*, 39924−39940.
(54) Hong, S. M., Park, C. W., Kim, S. W., Nam, Y. J., Yu, J. H., Shin, J. H., Yun, C. H., Im, S. H., Kim, K. T., Sung, Y. C., and Choi, K. Y. (2016) NAMPT suppresses glucose deprivation-induced oxidative stress by increasing NADPH levels in breast cancer. *Oncogene 35*, 3544−3554.
(55) Liu, X., Daskal, I., and Kwok, S. C. (2003) Effects of PTX1 expression on growth and tumorigenicity of the prostate cancer cell line PC-3. *DNA Cell Biol. 22*, 469−474.
(56) Browne, B. C., Hochgräfe, F., Wu, J., Millar, E. K., Barraclough, J., Stone, A., McCloy, R. A., Lee, C. S., Roberts, C., Ali, N. A., Boulghourjian, A., Schmich, F., Linding, R., Farrow, L., Gee, J. M., Nicholson, R. I., O'Toole, S. A., Sutherland, R. L., Musgrove, E. A., Butt, A. J., and Daly, R. J. (2013) Global characterization of signalling networks associated with tamoxifen resistance in breast cancer. *FEBS J. 280*, 5237−5257.
(57) Wang, W. H., Childress, M. O., and Geahlen, R. L. (2014) Syk interacts with and phosphorylates nucleolin to stabilize Bcl-x(L) mRNA and promote cell survival. *Mol. Cell. Biol. 34*, 3788−3799.
(58) Christensen, L. L., Holm, A., Rantala, J., Kallioniemi, O., Rasmussen, M. H., Ostenfeld, M. S., Dagnaes-Hansen, F., Øster, B., Schepeler, T., Tobiasen, H., Thorsen, K., Sieber, O. M., Gibbs, P., Lamy, P., Hansen, T. F., Jakobsen, A., Riising, E. M., Helin, K., Lubinski, J., Hagemann-Madsen, R., Laurberg, S., Ørntoft, T. F., and Andersen, C. L. (2014) Functional screening identifies miRNAs influencing apoptosis and proliferation in colorectal cancer. *PLoS One 9*, e96767.
(59) Nakakido, M., Tamura, K., Chung, S., Ueda, K., Fujii, R., Kiyotani, K., and Nakamura, Y. (2016) Phosphatidylinositol glycan anchor biosynthesis, class X containing complex promotes cancer cell proliferation through suppression of EHD2 and ZIC1, putative tumor suppressors. *Int. J. Oncol. 49*, 868−876.

DOI: 10.1021/acs.chemrestox.7b00269
Chem. Res. Toxicol. 2017, 30, 2187−2196

(60) Sareen, D., Darjatmoko, S. R., Albert, D. M., and Polans, A. S. (2007) Mitochondria, calcium, and calpain are key mediators of resveratrol-induced apoptosis in breast cancer. *Mol. Pharmacol. 72*, 1466−1475.
(61) Gong, B., Hu, H., Chen, J., Cao, S., Yu, J., Xue, J., Chen, F., Cai, Y., He, H., and Zhang, L. (2013) Caprin-1 is a novel microRNA-223 target for regulating the proliferation and invasion of human breast cancer cells. *Biomed. Pharmacother. 67*, 629−636.
(62) Rajan, R., Karbowniczek, M., Pugsley, H. R., Sabnani, M. K., Astrinidis, A., and La-Beck, N. M. (2015) Quantifying autophagosomes and autolysosomes in cells using imaging flow cytometry. *Cytometry, Part A 87*, 451−458.
(63) Hendershot, L. M. (2004) The ER function BiP is a master regulator of ER function. *Mt. Sinai J. Med. 71*, 289−297.
(64) Hou, S., Isaji, T., Hang, Q., Im, S., Fukuda, T., and Gu, J. (2016) Distinct effects of β1 integrin on cell proliferation and cellular signaling in MDA-MB-231 breast cancer cells. *Sci. Rep. 6*, 18430.
(65) Hu, Y., Sun, Z., Deng, J., Hu, B., Yan, W., Wei, H., and Jiang, J. (2017) Splicing factor hnRNPA2B1 contributes to tumorigenic potential of breast cancer cells through STAT3 and ERK1/2 signaling pathway. *Tumor Biol. 39*, 101042831769431.
(66) Belizzi, A., Greco, M. R., Rubino, R., Paradiso, A., Forciniti, S., Zeeberg, K., Cardone, R. A., and Reshkin, S. J. (2015) The scaffolding protein NHERF1 sensitizes EGFR-dependent tumor growth, motility and invadopodia function to gefitinib treatment in breast cancer cells. *Int. J. Oncol. 46*, 1214−1224.
(67) Genovese, G., Ghosh, P., Li, H., Rettino, A., Sioletic, S., Cittadini, A., and Sgambato, A. (2012) The tumor suppressor HINT1 regulates MITF and β-catenin transcriptional activity in melanoma cells. *Cell Cycle 11*, 2206−2215.
(68) Verdel, A., and Khochbin, S. (1999) Identification of a new family of higher eukaryotic histone deacetylases. Coordinate expression of differentiation-dependent chromatin modifiers. *J. Biol. Chem. 274*, 2440−2445.
(69) Tong, A., Zhang, H., Li, Z., Gou, L., Wang, Z., Wei, H., Tang, M., Liang, S., Chen, L., Huang, C., and Wei, Y. (2008) Proteomic analysis of liver cancer cells treated with suberonylanilide hydroxamic acid. *Cancer Chemother. Pharmacol. 61*, 791−802.
(70) Baumeister, P., Dong, D., Fu, Y., and Lee, A. S. (2009) Transcriptional induction of GRP78/BiP by histone deacetylase inhibitors and resistance to histone deacetylase inhibitor-induced apoptosis. *Mol. Cancer Ther. 8*, 1086−1094.
(71) Juengel, E., Meyer dos Santos, S., Schneider, T., Makarevic, J., Hudak, L., Bartsch, G., Haferkamp, A., Wiesner, C., and Blaheta, R. A. (2013) HDAC inhibition suppresses bladder cancer cell adhesion to collagen under flow conditions. *Exp. Biol. Med. (London, U. K.) 238*, 1297−1304.
(72) Dudakovic, A., Camilleri, E. T., Lewallen, E. A., McGee-Lawrence, M. E., Riester, S. M., Kakar, S., Montecino, M., Stein, G. S., Ryoo, H. M., Dietz, A. B., Westendorf, J. J., and van Wijnen, A. J. (2015) Histone deacetylase inhibition destabilizes the multi-potent state of uncommitted adipose-derived mesenchymal stromal cells. *J. Cell. Physiol. 230*, 52−62.

DOI: 10.1021/acs.chemrestox.7b00269
Chem. Res. Toxicol. 2017, 30, 2187−2196